A Backbone-Cyclic, Receptor 5-Selective Somatostatin Analogue: Synthesis, Bioactivity, and Nuclear Magnetic Resonance Conformational Analysis†

Chaim Gilon,‡ Martin Huenges,§ Barbara Mathä,§ Gary Gellerman,⊥ Vered Hornik,⊥ Michel Afargan,⊥ Oved Amitay,⊥ Ofer Ziv,⊥ Etty Feller,⊥ Asher Gamliel,⊥ Dvira Shohat,⊥ Mazal Wanger,⊥ Oded Arad,*,⊥ and Horst Kessler§

Department of Organic Chemistry, Hebrew University, Jerusalem, Israel, Institut für Organische Chemie und Biochemie, Technische Universität München, Lichtenbergstrasse 4, D-85747 Garching, Germany, and Peptor Ltd., Kiryat Weizmann, Rehovot 76326, Israel

Received September 19, 1997

Cyclo(PheN2-Tyr-D-Trp-Lys-Val-PheC3)-Thr-NH_2 (PTR 3046), a backbone-cyclic somatostatin analogue, was synthesized by solid-phase methodology. The binding characteristics of PTR 3046 to the different somatostatin receptors, expressed in CHO cells, indicate high selectivity to the SSTR5 receptor. PTR 3046 is highly stable against enzymatic degradation as determined in vitro by incubation with rat renal homogenate and human serum. The biological activity of PTR 3046 in vivo was determined in rats. PTR 3046 inhibits bombesin- and caerulein-induced amylase and lipase release from the pancreas without inhibiting growth hormone or glucagon release. The major conformation of PTR 3046 in CD_3OH, as determined by NMR, is defined by a type II′ β-turn at D-Trp-Lys and a cis amide bond at Val-PheC3.

Introduction

Backbone cyclization is a general method to introduce conformational constraints in peptides.[1−5] In backbone cyclization two amide nitrogens in the peptide backbone are involved in ring formation. These amide nitrogens are interconnected via a bridge consisting of alkyl groups and an amide bond or a disulfide bond. Using the backbone-cyclization approach, a variety of cyclic structures can be prepared for any given peptide sequence. These conformationally constrained peptidomimetic compounds can differ in the position of the ring (without affecting the presence of side-chain functional groups), in the size of the ring, and in the location and direction of the amide bond in the bridge.

Somatostatin-14 (SRIF) is a tetradecapeptide which inhibits the release of various hormones and enzymes.[6] It was first isolated as a growth hormone release inhibitor.[7] In addition to GH, SRIF inhibits the release of prolactin and ACTH from the pituitary, insulin and glucagon from the endocrine pancreas, and amylase and lipase from the exocrine pancreas.

SRIF exerts its action by interacting with G-protein-coupled, seven-transmembrane domain receptors. Five different SRIF receptors have been identified, cloned, and expressed individually. SRIF binds with high affinity to all five receptors. Octreotide (Sandostatin), a long-acting analogue of SRIF which is employed clinically for the treatment of acromegaly and in the treatment of tumors of the gastrointestinal tract, binds with high affinity to receptors 2 and 5 and with moderate affinity to receptor 3. Lanreotide and Vapreotide, two additional SRIF analogues currently in clinical development, have similar binding profiles to the five somatostatin receptors. No long-acting SRIF analogues have been reported that are specific for a single receptor of this family.[8]

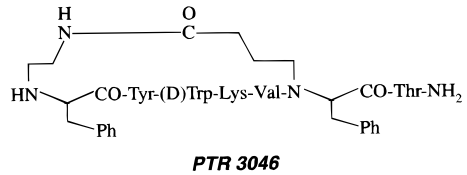

Figure 1. Structure of PTR 3046.

In this paper we describe the synthesis, bioactivity, and conformational analysis of PTR 3046, a metabolically stable, receptor 5-selective, backbone-cyclic somatostatin analogue of the sequence cyclo(PheN2-Tyr-D-Trp-Lys-Val-PheC3)-Thr-NH_2 (PheN2 is *N*-aminoethyl-Phe and PheC3 is *N*-carboxypropyl-Phe; the cyclization is carried out via a lactam bridge between these two N-alkylated residues) (Figure 1). Such a selective analogue could be useful in the treatment of pancreas-related and other GI related disorders.

Results and Discussion

Synthesis. The assembly of PTR 3046 was carried out by standard solid-phase techniques using Fmoc chemistry. Two N-alkylated Phe residues were incorporated in the sequence. The first, in position 6, contained a carboxypropyl group on the α-amino group

† Abbreviations: amino acid residues are designated according to the accepted three-letter codes; ACTH, adrenocorticotropic hormone; CHO, Chinese hamster ovary; DG, distance geometry; DMSO, dimethyl sulfoxide; ELISA, enzyme-linked immunosorbent assay; ESI-MS, electrospray ionization mass spectroscopy; GH, growth hormone; GI, gastrointestinal; HPLC, high-performance liquid chromatography; iv, intravenous; KLH, keyhole limpet hemocyanine; MALDI−TOF, matrix-assisted laser desorption−time-of-flight; MD, molecular dynamics; MS, mass spectroscopy; NMR, nuclear magnetic resonance spectroscopy; PheN2, N^a-(aminoethyl)Phe; PheC3, N^a(carboxypropyl)Phe; ROE, rotating frame Overhauser effect; ROESY, rotating frame Overhauser effect spectroscopy; sc, subcutaneously; SRIF, somatotrophin release inhibiting factor (native somatostatin); TFA, trifluoroacetic acid.

* To whom correspondence should be addressed.
‡ Hebrew University.
§ Technische Universität München.
⊥ Peptor Ltd.

S0022-2623(97)00633-X CCC: $15.00
Published on Web 02/24/1998

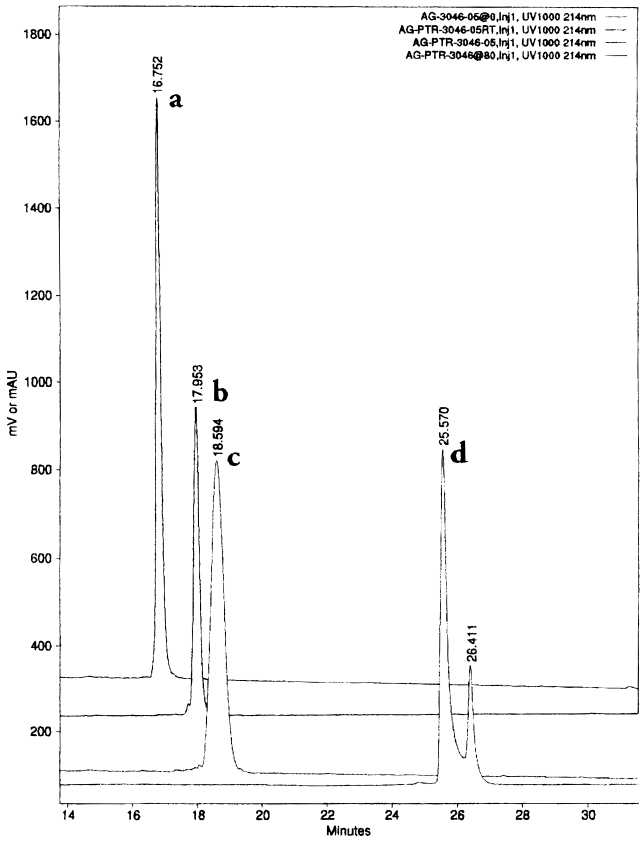

Figure 2. HPLC of PTR 3046 at (a) 80 °C, (b) 60 °C, (c) room temperature, and (d) 0 °C.

and the second, in position 1, an aminoethyl group. The carboxy and amino groups of these *N*-alkyl substituents were protected as their allyl and alloc derivatives, respectively. Following peptide synthesis, these allyl and alloc protecting groups were removed, and cyclization was carried out with the peptide attached to the polystyrene support. The cyclized peptide was cleaved from the solid support by reaction with TFA.

The crude peptide was purified by reversed-phase preparative HPLC. Fractions were analyzed by analytical HPLC, and relevant ones were combined. The product obtained from freeze-drying of the combined fractions showed a single peak in analytical HPLC. The HPLC chromatograms of PTR 3046 at various temperatures are shown in Figure 2. At room temperature the peak is broad. At 60 and 80 °C a sharp peak is observed, while at 0 °C the chromatogram consists of two peaks in a 70:30 ratio. The two peaks were collected and reanalyzed by HPLC. Both fractions exhibited the same peak pattern and the same temperature dependence as above. This is consistent with the presence of two interchanging conformations (see NMR conformational analysis below).

Edman degradation sequencing and amino acid analysis were consistent with the structure (the N-alkylated amino acids were not detected). Molecular weight of the product as determined by ESI-MS was in agreement with the calculated mass. MS/MS analysis of the peptide was also carried out (Figure 3); the fragmentations are consistent with the predicted molecular structure. Optical purity analysis of the amino acids of the peptide (carried out at C.A.T. GmbH in Germany) indicated very low levels of epimerization (here as well the N-alkylated amino acids were not determined). To rule out epimerization at position 1, the analogous peptide containing the D-PheN2 residue was prepared. This diastereomer is readily separable from PTR 3046 by HPLC upon co-injection.

Biological Activity. The affinity of PTR 3046 to the five somatostatin receptors was determined by a receptor binding assay in which the tested analogue competes with the binding of radiolabeled SRIF to cloned receptors expressed in CHO cells (Figure 4). (These measurements were carried out at Prof. Terry Reisine's laboratory, Department of Pharmacology, University of Pennsylvania School of Medicine, Philadalphia, PA, with the assistance of Dr. George Liapakis.) The curve corresponding to receptor 5 is for the human receptor; a very similar result was obtained with the rat receptor. Employing the average of several measurements and a linear regression plot,[9] we estimate an IC_{50} value of 67 nM for somatostatin receptor 5 and IC_{50} values above 1000 nM for somatostatin receptors 1−4. (SSTR1 and SSTR4 are the human receptors; SSTR2 and SSTR3 are the mouse receptors.)

The in vitro biostability of PTR 3046 was determined by incubation with human serum and rat renal homogenate. Figure 5 shows the biostability in renal homogenate, compared to Octreotide and SRIF. It can be seen that PTR 3046 is highly resistant to enzymatic degradation, in contrast to native SRIF. No degradation of PTR 3046 was seen after 18 h, while SRIF is degraded within minutes.

Physiological Efficacy. To correlate between in vitro receptor binding affinities and physiological activities, PTR 3046 was tested by a panel of in vivo assays in rats. These studies were based on the known activities of the native SRIF and the reference pharmaceutical compound Sandostatin.

1. Bombesin Model: In this model the release of pancreatic enzymes in rats is stimulated by administration of bombesin. A comprehensive study published by Coy et al.[10] suggested a possible correlation between activation of SSTR5 and the inhibitory effect of SRIF on the pancreatic exocrine secretion in this model.

In our study (Figure 6) it was shown that PTR 3046 as well as Octreotide inhibited pancreatic exocrine release. The two peptides were equipotent. A significant effect ($p < 0.05$) was found up to 90 and 120 min after subcutaneous injection of the peptides, indicating pharmacological long duration of action. Other peptides reported to inhibit pancreatic exocrine release are DC-23-99 and NC-8-12.[10] These somatostatin analogues, however, are not selective for SSTR5. In the experiments reported here the time course was measured at a single dose in order to determine the relevant potency of PTR 3046 to that of Octreotide.

2. Caerulein Model: This model differs from the bombesin model in the manner of stimulation of pancreatic exocrine release. Stimulation in this case was achieved with caerulein (a CCK analogue). The evaluation of exocrine release was based on the level of serum amylase and lipase activity. PTR 3046 as well as Sandostatin inhibited significantly the caerulein-induced exocrine release (Figure 7). The inhibitory effect was seen up to 2 h following sc administration of the peptides.

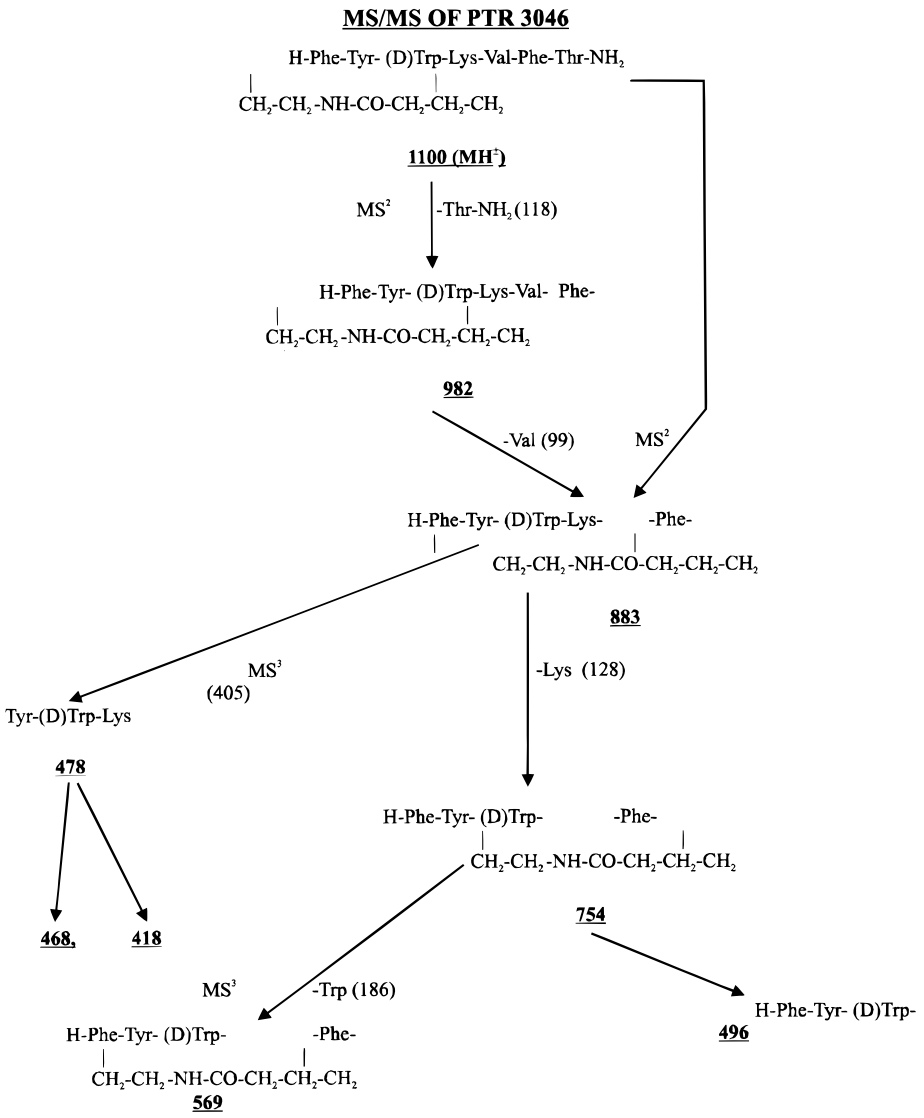

Figure 3. Analysis of fragmentation pattern of PTR 3046 by MS/MS.

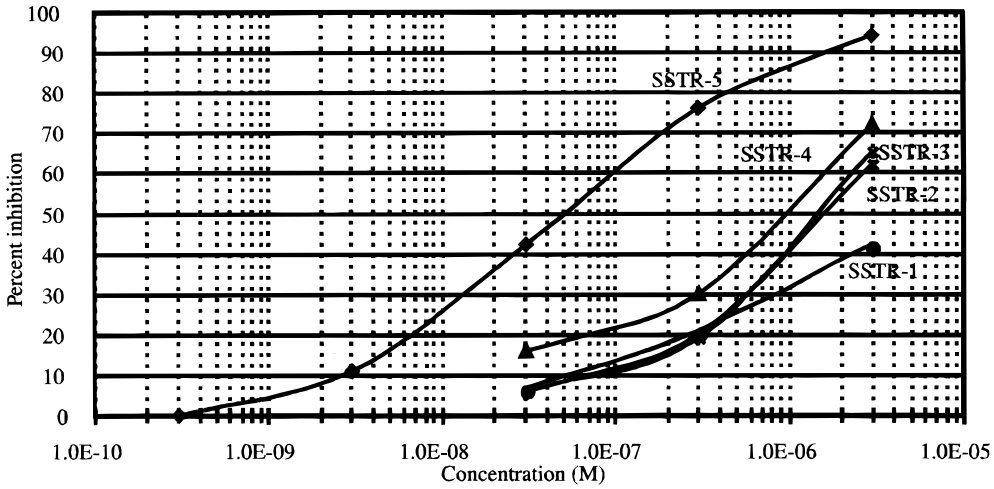

Figure 4. In vitro inhibition of SRIF binding to cloned SSTRs by PTR 3046.

3. Perfusion Model: In the bombesin and caerulein models described above, enzyme levels are determined in the serum. Amylase, for example, can also be released from salivary glands and other sites in the GI tract. A more direct measurement of pancreatic enzymes is the perfusion model. In this model levels of pancreatic enzymes are determined in a duodenal perfusate. Our results based on this model (Figure 8) indicate that both PTR 3046 and Octreotide (both administered by iv infusion) potently inhibit the pancreatic release of enzymes, as detected directly in the duodenal perfusate.

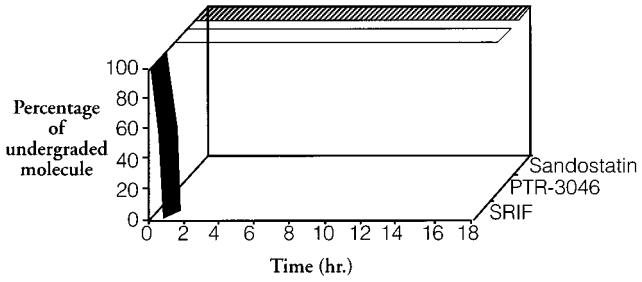

Figure 5. Metabolic biostability of PTR 3046 in renal homogenate, compared to Sandostatin and SRIF: (stippled bar, top) SRIF; (open bar, middle) PTR 3046; (solid bar, bottom) Sandostatin.

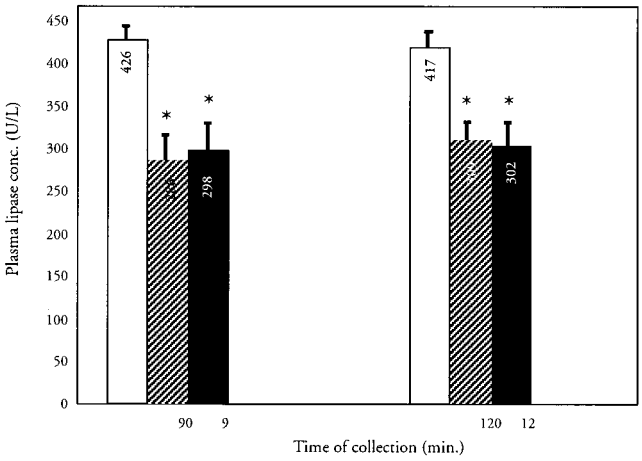

Figure 6. In vivo effect of PTR 3046 and Sandostatin on bombesin-induced exocrine release in rats (measured in serum): (solid bars, right) control (saline), $n = 9$; (stippled bars, middle) PTR 3046, 100 mg/kg, $n = 8$; (open bars, left) Sandostatin, 10 mg/kg, $n = 5$. An asterisk (*) denotes statistical significance ($p < 0.05$) in ANOVA.

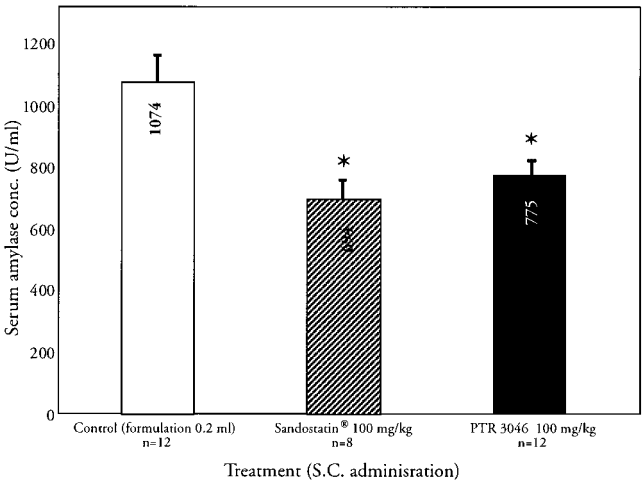

Figure 7. In vivo effect of PTR 3046 and Sandostatin on caerulein (2 h, iv infusion)-induced exocrine release in rats (measured in serum); *$p = 0.007$ (ANOVA).

4. Physiological Selectivity—GH and Glucagon Models: Figures 9 and 10 demonstrate the effects of the two somatostatin analogues on the release of GH and glucagon. As expected, Octreotide (which activates SSTR2, -3, and -5) was found to be a significant potent inhibitor ($p < 0.001$) on the release of GH and glucagon. In contrast to the effects of Octreotide on these endocrine profiles, PTR 3046 did not inhibit GH or glucagon release under the same experimental conditions. These results indicate a high physiological selectivity of PTR 3046 in vivo.

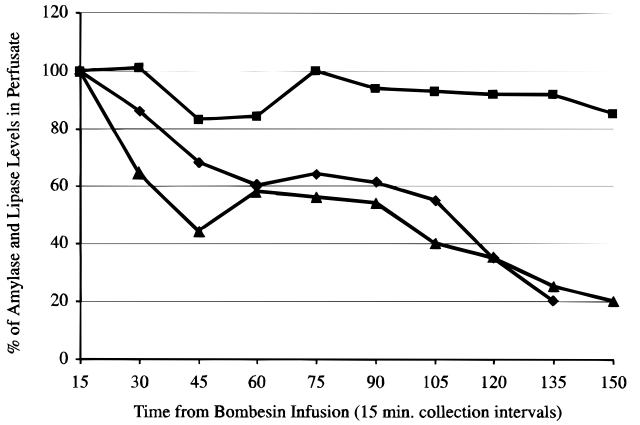

Figure 8. Effect of PTR 3046 and Sandostatin on pancreatic exocrine release in duodenal perfusion following bombesin induction (1 nmol/kg/h): (■) control (saline), $n = 10$; (▲) PTR 3046, 450 nmol/kg/h, $n = 6$; (●) Sandostatin, 300 nmol/kg/h, $n = 6$.

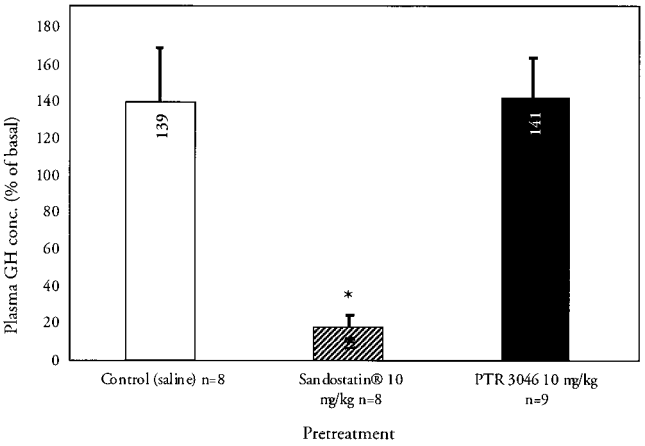

Figure 9. In vivo effect of PTR 3046 and Sandostatin on GH release in rats.

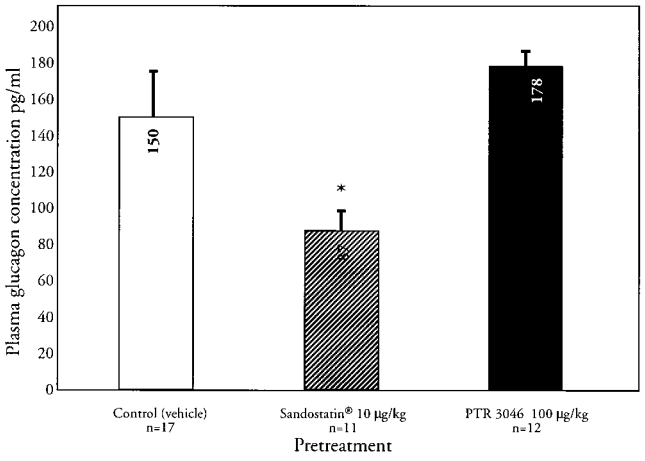

Figure 10. In vivo effect of PTR 3046 and Sandostatin on L-arginine glucagon release in rats.

5. Pharmacokinetic Properties of PTR 3046: The pharmacokinetics of PTR 3046 in rats was studied using an ELISA that was developed to measure this peptide. This assay is based on competition of the tested sample with the binding of specific polyclonal antibodies against

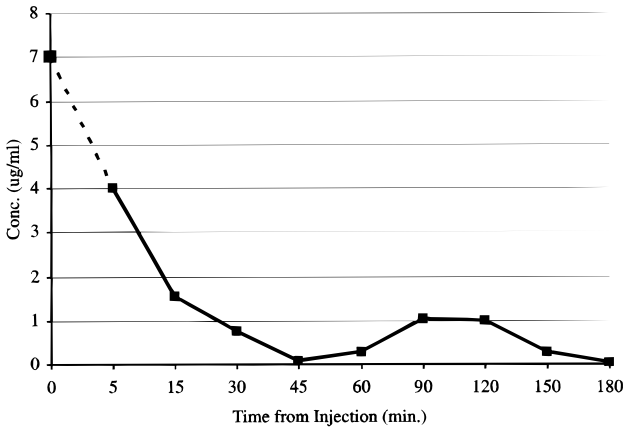

Figure 11. Plasma levels of PTR 3046 after iv bolus injection (100 mg, in rats) (ELISA).

PTR 3046 to absorbed peptide-conjugate. A pharmacokinetic profile of PTR 3046 in the blood following a bolus injection is shown in Figure 11. Based on the time course following an iv bolus administration of PTR 3046, its circulatory half-life in the rat was estimated to be about 15 min. A residual appearance in the plasma was detected at 90−120 min following the administration of the compound. The main route of elimination following iv administration was by biliary clearance, with additional renal clearance. An estimate of the half-life of this peptide in humans (based on metabolic differences between the species) is in the order of 1 h.

The results described above suggest that PTR 3046 has an affinity to SSTR5 and physiological duration of action similar to that of Sandostatin. However, PTR 3046 is selective and, unlike Sandostatin, does not interact with SSTR2.

6. Conformational Analysis: Structural investigations of PTR 3046 using 2D NMR and DG/MD techniques were performed as described previously.[12,13] Two conformations (cis/trans ratio, 60:40 for **1** and 20:80 for **2**) were observed for both **1** (TFA salt) and **2** (acetate salt) on the NMR shift time scale in CD_3OH at 300 K. For the dominant conformation of **1** and the minor conformation of **2**, a strong $Val^5H^\alpha/Phe^6H^\alpha$ ROE and the lack of Val^5H^α/IIH^α ROEs indicate a cis configuration of the amide bond between Val^5 and Phe^6. On the basis of the strong observed Val^5H^α/IIH^α ROE, the minor conformation of **1** and the dominant conformation of **2** appear to be all-trans. Obviously, the difference between the two salts is caused by the different degree of protonation at Phe^1NH. So, addition of TFA to the acetate salt causes a transition in the spectra from **2** to **1**.

The structures of both isomers of **1**, cis and trans, were determined using a combined approach of distance geometry (DG) and molecular dynamics calculations (MD). Taking advantage of its better sampling properties, we used DG calculations to generate a starting structure for subsequent MD calculations.

The resulting set of DG structures was analyzed for convergence. Since only the cis conformer of **1** shows convergence to a single conformation, the structure with the smallest total error was chosen for MD calculations. In the case of the trans conformer, no subsequent MD simulations were carried out since no unambiguous starting structure could be obtained. This could be due to high flexibility of the trans conformer.

The MD simulations for **1** (cis) were carried out in methanol, like the NMR investigations. The restraints (ROEs and coupling constants) were used for 100 ps of the simulation and then removed (free MD) for 100 ps to examine the quality of the structure. If the conformation developed from the restraints is not energetically favorable, significant conformational changes should occur during free MD.

The results are illustrated as averaged and energy-minimized structures from the 100-ps restrained MD calculations in Figure 12. The average distance violations are shown in Table 1. If diastereotopic assignment was not possible, the distance restraints were based on a pseudoatom placed between the corresponding protons. The highest restraint violations in **1** (cis) involve such pseudoatoms, and distances involving them are typically less accurate.

The averaged structure is characterized by a βII'-turn with D-Trp^3 in the $i+1$ position. It is well-known that a D-amino acid in position $i+1$ induces a βII'-turn.[14] The β-turn is accompanied by a hydrogen bond between the amide hydrogen of Val^5 and the carbonyl oxygen of Tyr^2, which is populated to 75% during the restrained MD. Furthermore an additional stabilizing hydrogen bond between Tyr^2 H^N and Val^5 C^O can be observed, a hydrogen-bonding pattern similar to the one found in β-sheets. The population of the observed hydrogen bonds is listed in Table 2.

An additional hydrogen bond is observed between the amide proton of Thr^7 and the carbonyl oxygen of Lys^4. This results in an orientation of the C-terminal amino acids toward the ring portion of the peptide. The small temperature shift of the amide proton of Thr^7 (−2.0 ppb/K) confirms this result. This back-folding also induces an overall bend conformation of the peptide backbone, as illustrated by Figure 13.

The simulation of the coupling constants, calculated from each structure of the trajectory and then averaged, is in good agreement with the experimental results except for the $^3J(H^N,H^\alpha)$ coupling constant of D-Trp^3 where the value differs by up to 2 Hz (Table 3).

Diastereotopic assignment of the D-Trp^3 H^β and Lys^4 H^β protons was possible. The side chains of D-Trp^3 and Lys^4 have a preferred orientation of $\chi_1 = 180°$ and $-60°$, respectively. According to the Pachler equations, these rotamers are populated 73% and 76%, respectively. The Val^5 side chain is oriented anti as the $^3J(H^\alpha,H^\beta)$ coupling constant of 15 Hz confirms.

The free MD simulation of **1** (cis) in methanol illustrates that the calculated conformation is predicted to be stable. The superposition of depicted conformations during the free MD shows that very few conformational changes took place and these mainly involve the ring linkage (Figure 14).

For **2**, DG calculations were performed for both the major and the minor conformation. No convergence was obtained in both cases. This might be due to the lower degree of protonation of the Phe^1 nitrogen because of the different pH of the counterion. This would lead to higher flexibility of the ring linkage so that the β-turn-stabilizing hydrogen bond between Tyr^2 H^N and Val^5 C^O could not be formed.

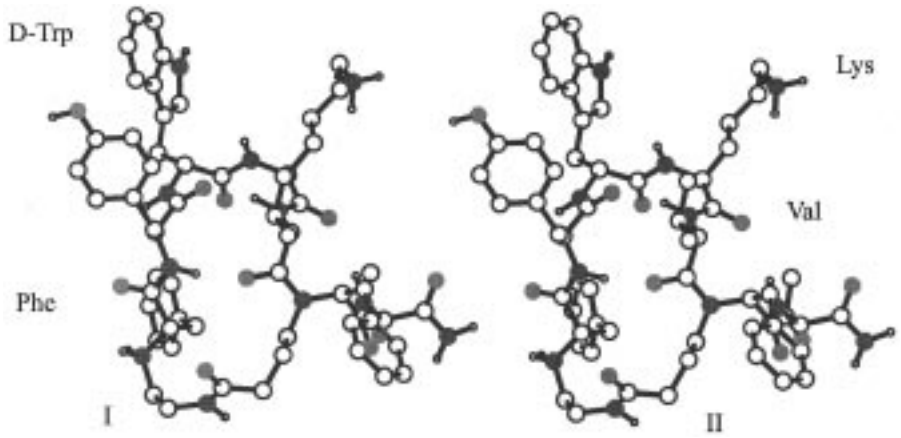

Figure 12. Stereoview of the averaged and energy-minimized conformation of **1** (cis) from a 100-ps restraint MD.

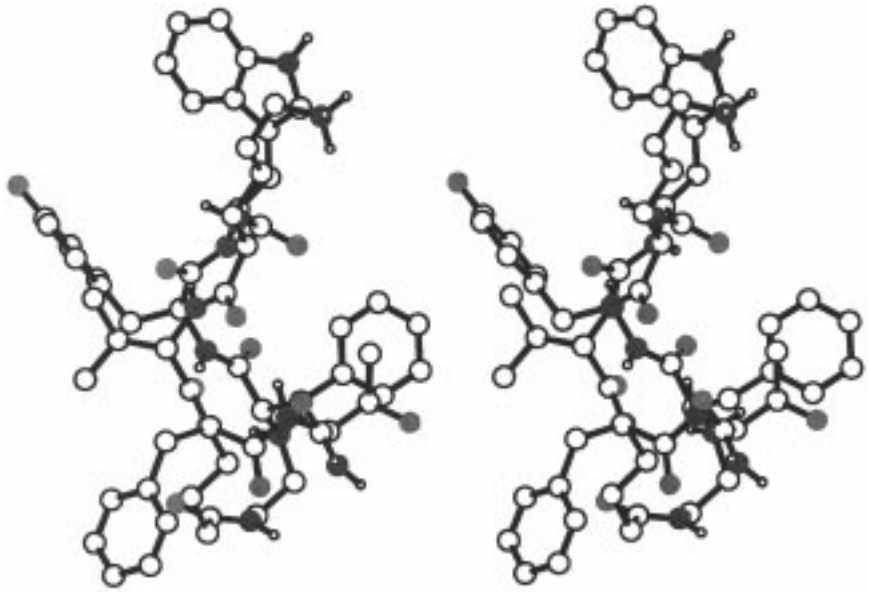

Figure 13. Stereoview of the side view of the averaged and energy-minimized conformation of **1** (cis).

Conclusion

We have prepared a receptor 5-selective, biostable, backbone-cyclic somatostatin analogue, PTR 3046. The selectivity toward SSTR5 was determined in vitro, by binding assays, to the five cloned, individually expressed receptors. PTR 3046 binds with similar affinity to human and rat SSTR5. The activity of PTR 3046 in vivo was determined in rats. PTR 3046 inhibits pancreatic exocrine secretion, but it does not inhibit pancreatic endocrine secretion or GH release from the pituitary. The conformation of PTR 3046 in CD_3OH solution was determined by NMR. The major conformation contains a type II′ β-turn at D-Trp-Lys and a cis amide bond at Val-PheC3. The availability of such a stable, selective analogue will assist in ascertaining the physiological roles of the SSTR5 receptor, as well as increase our understanding of structure−activity relationships in the somatostatin family. The physiological selectivity of PTR 3046, as seen in rats, suggests possible clinical applications of this compound in pancreatic and other GI-related disorders.

Experimental Section

Synthesis, Purification, and Analytical Chemistry. 1. Synthesis: Rink amide MBHA resin (1g) (NOVABiochem) (0.55 mmol/g) was preswollen for 1.5 h in NMP while shaking in a reaction vessel equipped with a sintered glass bottom. The Fmoc protecting group was removed from the resin by reaction with 20% piperidine in NMP (2 × 15 min, 5 mL each). Fmoc removal was monitored by the ninhydrin test (Kaiser test). A coupling cycle was carried out with Fmoc-Thr(OtBu)-OH (4 equiv), PyBrop (4 equiv), and DIEA (12 equiv) in NMP (5 mL) for 0.5 h at room temperature. Reaction completion was monitored by the qualitative ninhydrin test (Kaiser test). Following coupling the peptide-resin was washed with NMP (3 × 5 mL of NMP, 5 mL of DCM, and 5 mL of NMP for 2 min). Capping was carried out by reaction of the peptide-resin with acetic anhydride (capping mixture: HOAt (40 mg), NMP (5 mL), acetic anhydride (1 mL), DIEA (0.5 mL), and DMAP-(cat.)) for 0.5 h at room temperature. After capping NMP washes were carried out as above. Fmoc removal was carried out as described above. Fmoc-Phe(C3)-allyl BU was coupled (BU (2 equiv), PyBrop (2 equiv), DIEA (6 equiv), NMP (5 mL),0.5 h). Fmoc removal and the washing step were carried out as above. The peptide-resin was washed as above. The peptide-resin was reacted with Fmoc-Val-Cl (4 equiv, colidine (12 equiv), 1 h, 38 °C), and the coupling was repeated. Coupling completion was monitored based on the conversion of dipeptide to tripeptide (a sample of the peptide-resin was cleaved and the crude product was analyzed by HPLC). Fmoc removal was carried out as above. Fmoc-Lys(Boc)-OH was coupled to the peptide-resin by reaction conditions as for Fmoc-Thr(OtBu)-OH (see above). Coupling completion was monitored by ninhydrin test. Fmoc-D-Trp-OH was coupled to the

Table 1. ROESY-Derived Distances Compared to the Calculated Distances of 100-ps RMD Calculations of **1** (Cis Conformer)

atom 1	atom 2	$distance_{ROE}$ (pm)	$distance_{MD}$ (pm)
I H^N	I $H^{\alpha 1,2}$	292/237°	222[a]
I H^N	I $H^{\beta 2}$	356[a]	313[a]
I H^N	I $H^{\gamma 1,2}$	231/264[a]	248[a]
I H^N	I $H^{\beta 2}$	365[a]	350[a]
Phe[1] $H^{\beta 1/2}$	Phe[1] H^{α}	222[a]	215[a]
Phe[1] H^{α}	I $H^{\beta 2}$	278[a]	340[a]
Tyr[2] H^N	Phe[1] H^{α}	231	231
Tyr[2] H^N	Tyr[2] H^{α}	278	303
Tyr[2] H^N	Phe[1] $H^{\beta 1/2}$	249[a]	322[a]
Tyr[2] H^N	Phe[1] $H^{\beta 1}$	278/266[a]	299[a]
Tyr[2] H^N	I $H^{\beta 2}$	385	501
Tyr[2] H^N	Val[5] H^{β}	333	363
Tyr[3] H^N	Tyr[3] H^{α}	314	294
Tyr[3] H^N	Tyr[2] H^{α}	265	222
Tyr[3] H^N	Tyr[3] $H^{\beta 1}$	278	260
Tyr[3] H^N	Tyr[3] $H^{\beta 2}$	270	245
Tyr[3] H^{α}	Tyr[3] $H^{\beta 2}$	231	254
Lys[4] H^N	Lys[3] H^{α}	265	305
Lys[4] H^N	Trp[3] H^{α}	227	214
Lys[4] H^N	Lys[4] $H^{\beta 1}$	351	383
Lys[4] H^N	Lys[4] $H^{\beta 2}$	249	278
Lys[4] H^N	Lys[4] $H^{\gamma 1/2}$	273	296[a]
Lys[4] H^N	Val[5] H^N	263	256
Lys[4] H^{α}	Lys[4] $H^{\beta 1}$	222	239
Lys[4] H^{α}	Lys[4] $H^{\beta 2}$	246	305
Lys[4] H^{α}	Lys[4] $H^{\gamma 1/2}$	239	296[a]
Val[5] H^N	Val[5] H^{α}	264	299
Val[5] H^N	Lys[4] H^{α}	293	332
Val[5] H^N	Val[5] H^{β}	285	263
Val[5] H^N	Val[5] $H^{\gamma 1,2}$	240/334[a]	273[a]
Val[5] H^N	Lys[4] $H^{\beta 1}$	364	424
Val[5] H^N	Lys[4] $H^{\beta 2}$	357	347
Val[5] H^{α}	Phe[6] H^{α}	186	204
Val[5] H^{α}	Lys[4] $H^{\beta 1}$	244	444
Val[5] H^{α}	Val[5] $H^{\gamma 1,2}$	228/212	213[a]
Val[5] H^{β}	Phe[6] $H^{\beta 1,2}$	204/252	525[a]
Phe[6] H^{α}	Phe[6] $H^{\beta 1}$	204/241	208[a]
Thr[7] H^N	Thr[7] H^{α}	234	300
Thr[7] H^N	Thr[7] H^{β}	281	277
Thr[7] H^N	Phe[6] H^{α}	228	209
Thr[7] H^N	Phe[6] H^{β}	325[a]	355[a]
Thr[7] H^N	II $H^{\alpha 1}$	298[a]	447[a]
II $H^{\alpha 1}$	Phe[1] H^{α}	284[a]	350[a]

[a] The distances are measured toward a pseudoatom, which is placed between the two protons. This is necessary because no diastereotopical assignment is possible or the signals are not separated.

Table 2. Population of the Hydrogen Bonds during Restraint MD Calculations

donor	acceptor	population (%)
Val[5] H^N	Tyr[2] C^O	75
Tyr[2] H^N	Val[5] C^O	99
Thr[7] H^N	Lys[4] C^O	54

Table 3. Comparison of Measured and Calculated Proton Vicinal Coupling Constants of **1** (Cis Conformer)

	$^3J(H^N,H^{\alpha})$		$^3J(H^{\alpha},H^{\beta})$ (Hz)	
	exptl	calcd	exptl	calcd
Tyr[2]	10.3	10.2	8.7/7.3	
D-Trp[3]	8.5	6.3	10.6/2.2	12.1/5.5
Lys[4]	9.1	7.7	<1/11.0	4.9/12.4
Val[5]	9.2	8.4	15.1	
Phe[6]			8.2/8.2	
Thr[7]	8.3	8.0		

peptide-resin with PyBrop, as described above. Following Fmoc removal, Fmoc-Tyr(tBu)-OH was coupled in the same way. Following Fmoc removal, the second building unit was introduced: Fmoc-Phe-N2(alloc)-OH by reaction with PyBrop, as described for Fmoc-Phe(C3)-allyl B. The allyl and alloc protecting groups were removed by reaction with $Pd(PPh_3)_4$ and acetic acid (5%), *N*-methylmorpholine (2.5%) in chloroform under argon for 1.5 h at room temperature. The peptide-resin was washed as above. Cyclization was carried out with PyBOP, 3 equiv, DIEA, 6 equiv, in NMP, at room temperature for 0.5 h. The peptide-resin was washed as above. Following Fmoc removal the peptide-resin was washed (DCM, 3 × 5 mL), dried, and cleaved from the resin by reaction with TFA (94%), water (2.5%), EDT (2.5%), TIS (triisopropylsilane) (1%) at 0 °C for 15 min and for 1.5 h at room temperature. The mixture was filtered, and the resin was washed with a small volume of TFA. The filtrate was placed in a rotary evaporator, and all the volatile components were removed. An oily product was obtained. It was triturated with ether and the ether decanted. Yellow powder was obtained. This crude product was dried. The weight of the crude product was 290 mg.

2. Preparative Liquid Chromatography: A Waters Delta Prep 4000 preparative chromatography system connected to a Waters 486 UV−vis tunable absorbance detector and a waters fraction collector, controlled by a Millennium program (version 2.1), was used. A preparative HPLC column, 50 × 250 mm, C-18, 10−15 m (Vydac 218TP101550), was used to separate ca. 200 mg of crude material, dissolved in 30 mL of 80% A, 20% B (A, 0.1% trifluoroacetic acid (TFA) in HPLC pure water; B, 0.1% TFA in HPLC pure acetonitrile. The flow rate was 75 mL/min, starting with isocratic flow of 100% A for 10 min, then a linear gradient from 100% to 40% A in 20 min, followed by isocratic flow of 40%/60% A/B for 5 min, a linear gradient from 40% to 10% A in 15 min, again isocratic flow of 10%/90% A/B for 5 min, and finally a linear gradient from 10% to 100% A in 5 min. The column was then allowed to stabilize at 100% A for an additional 10 min. The detector was set at a wavelength of 214 nm. The fraction collector was set at a time mode of 10 s/fraction.

3. Analytical Liquid Chromatography: A Thermo Separation Products SpectraSystem P-4000 HPLC pump with an AS-3000 autosampler and a UV-1000 detector was used. An analytical column (4.6 × 250 mm, C-18, 5 m, Vydac 218TP54) was used, at 35 °C; mobile phase is A and B as above; flow rate, 1.0 mL/min (at 0 °C the flow rate was 0.5 mL/min). The sample (50 mL) was injected. After a 5-min equilibration period, the gradient started at an isocratic flow of 90% A for 1 min, followed by a linear gradient to 37% A in 30 min and to 10% A in an additional 5 min, followed by isocratic flow at 10%/90% A/B for 5 min, back with a linear gradient to 90% A in 5 min, and finally an isocratic flow of 90% A for 5 min. Detection was by absorbance at 214 nm.

4. Mass Spectrometry: MS was obtained with a VG-MALDI−TOF mass spectrometer (Altrincham, U.K.) as well as with a VG-Micromass Platform-II electrospray (ES) single-quadrupole mass spectrometer (Altrincham). Full scans were made from 200 to 2000 *m*/*z* (ESP+) (MCA); cone voltage was set at 80 V; scan time, 5.0 s; interscan time, 0.1 s; start time, 0.70 s; end time, 1.00 min; source temperature at 100 °C. For the MS/MS study a Finnigan Mat LCQ mass spectrometer (San Jose, CA) was used. With the built-in syringe pump the flow rate was set at 0.05 mL/min. The MS detector setting was at segment, 1; duration, 60.0 min; tune method, autotune; scan event, 3; all were positive. First event scan 250−1850 *m*/*z*; second event, Dep Zoom most intense ion from event 1; third event, Dep MS/MS most intense ion from event 1. On the dependent data settings: reject mass list, 279.00; parent mass list, none; subtracted mass, 0.00; default charge state, 2; isolation width, 2.00; collision energy, 35.00; minimum signal required, 250 000.

Amino acid analysis was carried out at Aminolab Ltd., Kiryat Weizmann, Rehovot, Israel. Sequencing was carried out at the Weizmann Institute of Science, Rehovot, Israel. Optical purity of amino acids was determined by Dr. Gerhardt at C.A.T. GmbH & Co. Chromatographie und Analsentechnik KG, Tübingen, Germany.

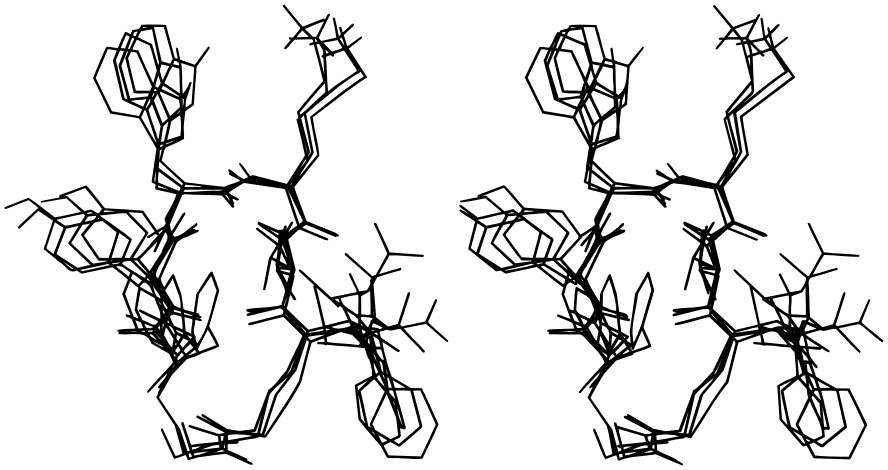

Figure 14. Superimposed conformations of **1** (cis) after 10, 30, and 50 ps of free MD.

Table 4. Proton Chemical Sifts (ppm) of **1** and **2** in CD_3OH at 300 K

peptide	residue	$H^N/H^{N\epsilon}$	H^α	H^β	H^γ	H^δ	H^ϵ
1							
			Major Conformation				
	I	8.50	3.67/3.20	3.11/2.35			
	Phe[1]	*a*	4.23	3.09			
	Tyr[2]	8.76	4.72	2.94/2.88			
	D-Trp[3]	8.92/10.34	4.40	3.24/3.11			
	Lys[4]	8.34/7.59	4.12	1.82/1.21	0.55	1.25	2.63/2.55
	Val[5]	8.68	4.38	2.59	0.99/0.61		
	Phe[6]		5.69	3.50/2.98			
	Thr[7]	8.01	4.18	4.05	0.90		
	II		3.80/3.54	2.08/1.91	2.51/2.10		
			Minor Conformation				
	I	8.02	3.33/3.22	2.90/2.81			
	Phe[1]	*a*	3.92	3.13/3.02			
	Tyr[2]	8.53	4.24	2.69			
	D-Trp[3]	7.97/10.28	4.68	3.09			
	Lys[4]	7.62/*a*	4.44	1.72/1.60	1.20	1.59	2.84
	Val[5]	8.07	4.48	1.92	0.92		
	Phe[6]		4.34	3.44/3.36			
	Thr[7]	7.44	4.17	4.28	1.12		
	II		3.45/2.77	1.82	2.18		
2							
			Major Conformation				
	I	7.68	3.08/3.02	2.42/2.33			
	Phe[1]	*a*	3.18	2.87/2.55			
	Tyr[2]	8.12	4.36	2.77/2.67			
	D-Trp[3]	8.02	4.63	3.14/3.10			
	Lys[4]	7.82/*a*	4.37	1.67/1.53	1.15	1.52	2.81
	Val[5]	8.02	4.38	1.90	0.93/0.84		
	Phe[6]		4.33	3.41/3.35			
	Thr[7]	7.35	4.16	4.29	1.09		
	II		3.33/2.76	1.82	2.21/2.10		
			Minor Conformation				
	I	7.90	3.43/2.93	2.54/2.45			
	Phe[1]	*a*	3.37	2.67			
	Tyr[2]	8.13	4.37	2.77/2.67			
	D-Trp[3]	7.96	4.39	3.07			
	Lys[4]	8.09/*a*	4.29	1.79/1.42	0.92	1.40	2.70
	Val[5]	8.47	4.46	1.91	0.90/0.68		
	Phe[6]		5.24	3.40/2.88			
	Thr[7]	8.25	4.17	4.05	1.06		
	II		3.72/3.41	1.79	2.15/2.11		

[a] Could not be unambiguously assigned.

Receptor Binding Assays. The affinity of the somatostatin analogue for the receptors was tested in a competition assay with [^{125}I]Tyr^{11}-SRIF (based on the method described by Raynor et al.[11]) to membrane preparations of CHO cells stably expressing the somatostatin receptors (hSSTR1, mSSTR2, mSSTR3, hSSTR4, hSSTR5, and rSSTR5). In summary, cell membranes were homogenated in Tris buffer in the presence of protease inhibitors and incubated for 30−40 min with [^{125}I]Tyr-SRIF and different concentrations of the tested sample. The binding reactions were filtered, the filters were washed, and the bound radioactivity was counted in a γ-counter. Nonspecific binding was defined as the radioactivity remaining

Table 5. Carbon Chemical Sifts (ppm) of **1** and **2** in CD_3OH at 300 K

peptide	residue	C^α	C^β	C^γ	C^δ	C^ϵ
1						
		Major Conformation				
	I	39.0	49.8			
	Phe[1]	63.8	38.8			
	Tyr[2]	55.4	37.9			
	D-Trp[3]	57.8	26.9			
	Lys[4]	53.4	30.3	22.5	30.3	40.0
	Val[5]	57.3	31.4	19.2/18.9		
	Phe[6]	63.1	37.1			
	Thr[7]	59.7	67.9	*a*		
	II	43.8	25.9	34.1		
		Minor Conformation				
	I	38.1	49.5			
	Phe[1]	62.7	37.8			
	Tyr[2]	57.8	36.4			
	D-Trp[3]	54.9	27.7			
	Lys[4]	53.4	32.6	23.2	27.9	44.5
	Val[5]	56.1	22.1	22.1	19.8/17.9	
	Phe[6]	65.7	35.3			
	Thr[7]	60.4	67.8	20.3		
	II	50.7	35.3	32.6		
2						
		Major Conformation				
	I	40.1	48.4			
	Phe[1]	64.8	40.3			
	Tyr[2]	57.0	37.5			
	D-Trp[3]	54.8	27.5			
	Lys[4]	53.5	32.4	23.1	27.9	40.4
	Val[5]	55.9	31.4	17.9/19.8		
	Phe[6]	65.3	35.1			
	Thr[7]	60.7	67.7	20.2		
	II	50.3	25.5	33.5		
		Minor Conformation				
	I	40.2	47.8			
	Phe[1]	*a*	*a*			
	Tyr[2]	*a*	*a*			
	D-Trp[3]	57.0	27.5			
	Lys[4]	53.5	31.4	23.1	27.5	40.2
	Val[5]	56.4	29.8	18.3/19.7		
	Phe[6]	62.2	36.8			
	Thr[7]	60.7	68.1	20.6		
	II	43.0	25.5	35.0		

[a] Could not be unambiguously assigned.

bound in the presence of 1 μM unlabeled SRIF-14. The IC_{50} values presented are the concentrations required to reduce SRIF binding to 50% of the maximum.

ELISA for PTR 3046. Polyclonal antibodies against PTR 3046 were developed in rabbits immunized with the peptide conjugated with KLH. For the assay, ELISA plates were coated with 3 mg/mL peptide-tyroglobulin conjugate and blocked with 3% BSA/PBS + 0.05% Tween-20. Serum samples were mixed with 1:10 000 dilution of the rabbit anti-PTR 3046 serum and then transferred to the ELISA plate. Unbound antibody was removed by washing. To detect bound antibody, 1:1000 dilution of anti-rabbit antibodies conjugated with alkaline phosphatase (Sigma, Israel) was added to all wells, incubated, and washed. The signal was then developed by incubation with PNPP substrate. Product accumulation was determined by optical absorption at 405 nm. The assay was calibrated against a series of known dilutions of the peptide.

Stability of PTR 3046. The biostability of PTR 3046 was studied in rat kidney homogenate. Peptides were incubated at 37 °C in homogenate, and samples were collected at specified time points for evaluation of the undegraded peptide by HPLC analysis.

Animal Studies. In vivo studies were performed on Wistar male rats (Harlan, Israel). Animals were fasted overnight. Tests were carried out under nembutal anesthesia (60 mg/kg ip). Drugs were administered by either subcutaneous bolus injection or intravenous infusion. Blood was collected from the right external jugular vein, except for the glucagon tests, where blood was obtained from the portal vein. Hormones were measured in plasma samples by rat specific RIA kits. Enzymes were measured by calorimetric assays based on enzymatic activity.

GH and Glucagon Tests. Animals anesthetized with nembutal were used for the GH and glucagon release studies. Drugs were administered sc 10 min following anesthesia. After an additional 20 min, femoral cannulation was performed, and 0.6 mg/kg L-Arg was administered intravenously in order to stimulate glucagon release. Blood was collected 5 min following L-Arg stimulation from the portal vein for glucagon and from the abdominal vena cava for GH measurements. Plasma was obtain from blood samples and maintained at −20 °C until assay.

Determination of Plasma Amylase and Lipase. Two jugular vein cannulations were performed under anesthesia. Bombesin or caerulein infusion of 50 or 4 nM/kg/h, respectively, was started. Blood was collected after 90 and 120 min of infusion. Plasma was obtained, and enzymes were determined as activity units/mL of plasma.

Duodenal−Pancreatic Perfusion. The duodenal segment which drains the pancreas was dissociated proximally from the stomach and distally from the jejunum. The segment was perfused with physiological saline solution, and pefusate was collected at 15-min time points. Stimulation of pancreatic release was done by iv infusion of bombesin or caerulein, 1 or 4 nM/kg/h, respectively. As soon as enzyme levels had reached a constant value during perfusion, drugs were infused iv for an additional period of 2 h. Pancreatic enzyme levels were measured in the perfusate samples. The data are presented

Table 6. Proton Vicinal Coupling Constants $^3J_{HN/H_\alpha}$ and $^3J_{H_\alpha/H_\beta}$ (Hz) of **1** and **2**

peptide	type[a]	I	Phe[1]	Tyr[2]	D-Trp[3]	Lys[4]	Val[5]	Phe[6]	Thr[7]
1									
				Major Conformation					
	HN/H^α	5.9/7.6	*c*	10.3	8.5	9.1	9.2		8.3
	H^α/H^α	*b*	*b*	8.7/7.3	10.6/2.2	<1/11.0	15.1	8.2/8.2	*b*
				Minor Conformation					
	HN/H^α	7.1/7.4	*c*	7.1	8.5	8.1	9.3		8.4
	H^α/H^α	*b*	5.2/9.1	*b*	*b*	5.0/7.9	15.6	6.8/7.7	*b*
2									
				Major Conformation					
	HN/H^α	5.6/6.1	*c*	*b*	8.4	6.4	7.9		9.8
	H^α/H^α	*b*	5.6/8.7	*b*	*b*	<1/8.8	16.2	6.2/6.3	8.1
				Minor Conformation					
	HN/H^α	8.0/3.3	*b*	*b*	*b*	8.7	7.9		7.9
	H^α/H^α	*b*	*b*	*b*	*b*	<1/9.3	13.1	9.2/5.7	7.0

[a] First value for low-field signal, second value for high-field signal. [b] Signals overlapped, coupling constants not determined. [c] H^N not assigned.

Table 7. Temperature Dependence of the Amide Protons of **1**[a]

conformer	I	Tyr[2]	D-Trp[3]	Lys[4]	Val[5]	Thr[7]
major	−6.0	−6.2	−11.0	−8.2	−6.0	−2.0
minor	−5.6	−10.4	−9.2	−3.6	−9.0	−2.0

[a] Coefficients given in ppb/K.

as percentage of measured enzyme levels compared to initial constant level after bombesin stimulation.

Pharmacokinetic Properties. An in vivo pharmacokinetic model was developed in male Wistar rats (350−400 g). Right external jugular vein cannulation was done under light ether anesthesia, and animals were allowed 24 h recovery from cannulation. On the day of the experiment, PTR 3046 was administered to the conscious rats as an intravenous bolus injection (250 μg/kg). Blood samples (0.3 mL) were collected at specified intervals from the iv catheter. Samples were kept in plastic tubes containing 15 U/mL heparin and kept on ice. Plasma heparin was extracted by centrifugation (1500g × 10 min). At the end of each time course, urine was collected under light ether stimulation. Samples were kept at −20 °C until further analysis by ELISA.

Statistical Method. Plasma hormone concentrations were expressed as means and standard error of the means (mean ± SEM). One-way ANOVA followed by Fisher's contrast was used to compare between groups. A p value of <0.05 was considered statistically significant. Animals were assigned to the various groups (i.e., control, experimental, etc.) randomly.

NMR Measurements. All NMR spectra were recorded on Bruker DMX600 and DMX750 spectrometers and processed on Silicon Graphics workstations with the UXNMR software package. The measurements were performed at 300 K using an 18 or 20 mM solution, respectively, of peptides **1** and **2** in CD_3OH. Assignment of resonances (cf. Tables 4 and 5) and determination of interproton distances (cf. Table 1) were done by standard 2D NMR techniques (TOCSY, PECOSY, ROESY with a pulsed spin−lock, HMQC, HMQC-TOCSY). All chemical shifts are referenced to the CD_3OH signal at 3.30 ppm (^{1}H) and 49.0 ppm (^{13}C).

Distance information for the structure investigation in DMSO was derived from a ROESY spectrum with mixing times of 150 ms. For correct conversion of measured ROESY integral volumes to distance constraints, the offset effect was taken into account using the isolated two-spin approximation (ISPA).[15] $^3J_{NH/H\alpha}$ (using the method of Kim and Prestegard[16]) and $^3J_{H\alpha/H\beta}$ coupling constants (cf. Table 6) were obtained from the PECOSY spectra. Temperature coefficients (cf. Table 7) for **1** were determined between 300 and 320 K in steps of 5 degrees.

Computational Procedures. The structure calculations were performed on a Silicon Graphics Crimson R4000. Distance geometry calculations were carried out using a modified version[17] of DISGEO.[18] The DG procedure was started with the embedding of 100 structures using random metrization.[19] For the refinement of the structures, DISGEO employs distance- and angle-driven dynamics with ROE restraints and an additional harmonic ^3J coupling potential according to the Karplus equation. From the resulting 100 structures, 10−20 low-error structures were examined. If convergence was achieved, the conformation with the smallest total error was chosen for subsequent MD calculations.

The MD calculations were carried out with the program DISCOVER 95.0 using the CVFF89 force field.[20] The DISCOVER 95.0 program was modified to take coupling constants into account as additional harmonic restraints according to the Karplus equation. The lowest-error structure of the previous DG calculation was placed in a cubic box with a box length of 35 Å and periodic boundary conditions, filled with methanol. During the MD calculations a time step of 1 fs was employed. The minimization process was subdivided into two steps. First the solute was fixed, and then all atoms were allowed to move freely. After this the system was heated gradually starting from 50 K and increasing in 2-ps steps gradually to 300 K, by direct scaling of velocities. The system was equilibrated for 20 ps with temperature coupling. Subsequently, configurations were saved every 100 fs for another 100 ps. During this part of the simulation, distance restraints and coupling restraints were applied with a force constant of 1.0 and 0.3 kcal/mol Å, respectively. The averaged structure of the restrained MD was minimized by using the method of steepest descent. The distance violations were calculated using a $<r^{-3}>^{-1/3}$ formula. The MD calculation was continued without restraints for another 100 ps with the sampling rate unchanged.

Acknowledgment. The authors would like to thank Prof. Terry Reisine and Dr. George Liapakis, Department of Pharmacology, University of Pennsylvania School of Medicine, for their assistance in the binding assays. We also wish to thank Mrs. Mor Cohen for her excellent artwork in the preparation of the figures.

References

(1) Gilon, C.; Halle, D.; Chorev, M.; Selinger, Z.; Byk, G. Backbone cyclization: A new method for conferring conformational constraint on peptides. *Biopolymers* **1991**, *31*, 745−750.
(2) Bitan, G.; Behrens, S.; Matha, B.; Mashriki, Y.; Hanani, M.; Kessler, H.; Gilon, C. New backbone cyclic substance P analogues. *Lett. Pept. Sci.* **1995**, *2*, 121−124.
(3) Byk, G.; Gilon, C. Building units for N-backbone cyclic peptides. 1. Synthesis of protected N−(ω-aminoalkylene)amino acids and their incorporation into dipeptide units. *J. Org. Chem.* **1992**, *57*, 5687−5692.
(4) Saulitis, J.; Mierke, D. F.; Byk, G.; Gilon, C.; and Kessler, H. Conformation of cyclic analogues of substance P: NMR and molecular dynamics in dimethyl sulfoxide. *J. Am. Chem. Soc.* **1992**, *114*, 4818−4827.
(5) Grdadolnik, S. G.; Mierke, D. F.; Byk, G.; Zeltser, I.; Gilon, C.; Kessler, H. Comparison of the conformation of active and nonactive backbone cyclic analogues of substance P as a tool to elucidate features of the bioactive conformation: NMR and molecular dynamics in DMSO and Water. *J. Med. Chem.* **1994**, *37*, 2145−2152.
(6) (a) Reichlin, S. Somatostatin: Historical aspects. *Scand. J. Gastroenterol.* **1986**, *21* (Suppl. 119), 1−10. (b) *Somatostatin and Its Receptors*; Chadwick, D. J., Cardew, G., Eds.; Ciba Foundation Symposium 190; John Wiley & Sons: New York, 1995.
(7) Brazeau, P.; Vale, W. W.; Burgus, R.; Ling, N.; Butcher, M.; Rivier, J.; Guillemin, R. Hypothalamic polypeptide that inhibits the secretion of immunoreactive pituitary growth hormone. *Science* **1973**, *179*, 77−79.
(8) Patel, Y. C.; Srikant, C. B. Subtype selectivity of peptide analogues for all five cloned human somatostatin receptors (hsstr 1−5). *Endocrinology* **1994**, *135*, 2814−2817.
(9) Limbird, L. E., *Cell Surface Receptors: A Short Course on Theory and Methods*; Kluwer Academic Publishers: Boston.
(10) Coy, D. H.; Rossowski, W. J. Somatostatin analogues and multiple receptors: Possible physiological roles. In *Somatostatin and Its Receptors*; Ciba Foundation Symposium 190; John Wiley & Sons: New York, 1995; Chadwick, D. J., Cardew, G., Eds.; pp 240−254.
(11) Raynor, K.; Murphy, W.; Coy, D.; Taylor, J.; Moreau, J.-P.; Yasuda, K.; Bell, G. I.; Reisine, T. *Mol. Pharmacol.* **1993**, *43*, 838−844.
(12) Kessler, H.; Seip, S. NMR of peptides. In *Two-Dimensional NMR Spectroscopy: Applications of Chemists and Biochemists*; Croasmun, W. R., Carlson, R. M. K., Eds.; VCH Publishers: New York, 1994; p 619.
(13) Eberstadt, M.; Gemmecker, G.; Mierke, D. F.; Kessler, H. Scalar coupling constants-Their analysis and their application for the elucidation of structures. *Angew. Chem., Int. Ed. Engl.* **1995**, *34*, 1671−1695.
(14) Kessler, H.; Bats, J. W.; Griesinger, C.; Knoll, S.; Will, M.; Wagner, K. Conformational analysis of a superpotent cycloprotective cyclic Somatostatin analogue. *J. Am. Chem. Soc.* **1988**, *110*, 1033−1049.
(15) Neuhaus, D.; Williamson, M. *The Nuclear Overhouser Effect in Structural and Conformational Analysis*; VCH Publishers: New York, 1989.
(16) Kim, Y.; Prestegard, J. H. Measurement of vicinal couplings from cross peaks in COSY spectra. *J. Magn. Reson.* **1989**, *84*, 9−13.
(17) Mierke, D. F.; Kessler, H. Improved molecular dynamics simulations for the determination of peptide structures. *Biopolymers* **1993**, *33*, 1003−1017.

(18) (a) Havel, T. F. DISGEO; Quantum Chemistry Exchange Program, Exchange No. 507; Indiana University, 1988. (b) Havel, T. F. An evaluation of computational strategies for use in the determination of protein structure from distance constraints obtained by nuclear magnetic resonance. *Prog. Biophys. Mol. Biol.* **1991**, *56*, 43−78. (c) Crippen, G. M.; Havel, T. F. *Distance Geometry and Molecular Conformations;* Research Studies Press Ltd., John Wiley & Sons: Somerset, England, 1988. (d) Havel, T. F.; Wüthrich, K. A distance geometry program for determining the structures of small proteins and other macromolecules from nuclear magnetic resonance measurements of intramolecular 1H-1H proximities in solution. *Bull. Math. Bio.* **1984**, *46*, 673−698.

(19) Havel, T. F. The sampling properties of some distance geometry algorithms applied to unconstrained polypeptide chains: A study of 1830 independently computed conformations. *Biopolymers* **1990**, *29*, 1565−1585.

(20) (a) Hagler, A. T.; Lifson, S.; Dauber, P. A benchmark for the objective comparison of alternative force fields. *J. Am. Chem. Soc.* **1979**, *101*, 5122−5130. (b) DISCOVER, Version 95.0; BIOSYM Technologies, 10065 Barnes Canyon Rd, San Diego, CA 92121.

JM970633X